Nuclear foci of mammalian recombination proteins are located at single-stranded DNA regions formed after DNA damage

ELKE RADERSCHALL*, EFIM I. GOLUB†, AND THOMAS HAAF*‡

*Max Planck Institute of Molecular Genetics, Ihnestrasse 73, 14195 Berlin, Germany; and †Department of Genetics, Yale University School of Medicine, New Haven, CT 06520

ABSTRACT A sensitive and rapid *in situ* method was developed to visualize sites of single-stranded (ss) DNA in cultured cells and in experimental test animals. Anti-bromodeoxyuridine antibody recognizes the halogenated base analog incorporated into chromosomal DNA only when substituted DNA is in the single strand form. After treatment of cells with DNA-damaging agents or γ irradiation, ssDNA molecules form nuclear foci in a dose-dependent manner within 60 min. The mammalian recombination protein Rad51 and the replication protein A then accumulate at sites of ssDNA and form foci, suggesting that these are sites of recombinational DNA repair.

Eukaryotic cells are endowed with multiple pathways to repair damaged DNA. One of the major pathways is nucleotide excision repair, which can remove a broad range of DNA lesions. Nucleotide excision repair excises oligonucleotides of 25–32 bp including the damaged DNA, filling in the single-stranded (ss) DNA gap (1). This process is very efficient and usually repairs most DNA lesions before the damaged region is replicated. However, if the replication fork meets unrepaired DNA damage, breaks may occur in one or both strands of the nascent DNA (2). Single- and double-strand breaks (DSBs) may also arise as a direct effect of many DNA-damaging agents such as ionizing radiation. Single-strand breaks are efficiently repaired and do not represent a threat for cell survival. In contrast, DSBs are potentially lethal. DSBs may be repaired either by direct end-joining of the broken ends in a process that is mediated by the Mre11–Rad50 complex or by homologous recombination (3). In yeast, DSBs are mainly repaired by homologous recombination; genes of the *Rad52* epistasis group are largely responsible for this pathway. Although mammalian cells are presumed to repair DSBs predominantly by nonhomologous end-joining (4, 5), accumulating experimental evidence suggests that homologous recombination also plays an essential role in mammalian DSB repair (6–8).

DSB repair by homologous recombination starts with 5′ to 3′-exonucleolytic digestion of one DNA strand, which leads to the formation of 3′-overhanging ssDNA tails. In *Escherichia coli*, this ssDNA associates with the RecA recombination enzyme, forming the ssDNA–RecA filament. This RecA–nucleoprotein filament promotes homology search by the single DNA strand and initiates the exchange between ssDNA and homologous double-stranded (ds) DNA (3, 9). Rad51 is a structural and functional eukaryotic homolog of *E. coli* RecA (10, 11). Similar to RecA, both yeast and mammalian Rad51 proteins form nucleoprotein filaments on ssDNA, mediating homologous pairing and strand-exchange reactions between ssDNA and homologous dsDNA (12–15). Homologous pairing and DNA-strand exchange mediated by Rad51 are facilitated *in vitro* by the ssDNA-binding protein, RPA (12, 16–18).

In normal, cultured human cells, the HsRad51 protein is detected in multiple discrete foci in the nucleoplasm of a low number of cells by immunofluorescent antibodies. After DNA damage the percentage of cells with focally concentrated Rad51 protein increases in a time- and dose-dependent manner. The same cells show unscheduled DNA repair synthesis (19, 20). The DNA damage-induced redistribution of Rad51, a protein that *in vitro* mediates search for homology and strand exchange, suggests a role for Rad51 in recombinational DNA repair. Because mammalian Rad51 protein is also highly enriched in discrete nuclear foci during meiotic prophase, it may be involved in meiotic recombination as well (19, 21, 22). In addition, cytological and genetic studies in yeast have clearly demonstrated that the Rad51 gene is required during meiosis (10, 23, 24).

In this paper we describe a very simple and fast assay that allows visualization and quantification of ssDNA regions in individual cells. This assay can provide valuable information on DNA damage and mammalian DNA repair pathways. By using this assay, we found that mammalian recombination proteins, Rad51 and RPA, associate with long stretches of ssDNA that appear after treatment of cells with DNA-damaging agents.

MATERIALS AND METHODS

Cell Substrates. Strains PPL and KRA are primary human fibroblast cultures. TGR-1 cells are rat fibroblasts. XPA is a simian virus 40-transformed fibroblast line derived from a patient with the recessive hereditary disorder Xeroderma pigmentosum group A (XPA). Because XPA and BrdUrd-substituted normal cells are sensitive to daylight and luminescence from most lamps, they were grown in flasks that were wrapped with tin foil.

Induction of ssDNA in Cultured Cells After DNA Damage. Monolayer cells were grown for 30 hr in DMEM medium (GIBCO) containing 10 μg/ml BrdUrd. Then the BrdUrd was washed out and BrdUrd-free medium was added. To induce DSBs in DNA, 0.5 μg/ml mitomycin C (MMC) or 0.5–20 μg/ml etoposide were added to the new culture medium for 1 hr. Alternatively, cells were exposed to a Cobalt 60 (^{60}Co) irradiator at doses of 0.5–10 Gy. To allow for the processing of DSBs and DNA repair to occur, the treated cells were washed with and then cultured for various times in drug-free medium. In control experiments, cultures were treated with 10 μg/ml cycloheximide or 100 ng/ml actinomycin D for 1 hr, which kill cells by inhibiting protein synthesis and transcription. Cells were detached from culture flasks by gentle trypsination, pelleted, and resuspended in PBS (136 mM NaCl/2 mM KCl/10.6 mM Na$_2$HPO$_4$/1.5 mM KH$_2$PO$_4$, pH 7.3) prewarmed at 37°C.

Visualization of ssDNA in Meiotic Cells. The cycle time to produce spermatozoa from premeiotic cells in mice is approxi-

mately 5 weeks. To label DNA of all spermatogenic cell types with BrdUrd, male mice were supplied with drinking water containing 0.5 mg/ml BrdUrd continuously for more than 6 weeks (25, 26). Immediately after the BrdUrd-treated mouse was sacrificed, the testes and the cauda epididymis were removed and placed in PBS. The testicular tissue was cut into small pieces and the seminiferous tubules were emptied by squeezing with fine forceps. The resulting cell suspension was transferred to a 15-ml centrifuge tube and allowed to settle for 10 min. The supernatant was then carefully removed with a pipette and transferred to a new centrifuge tube. The density of testicular cells in PBS was adjusted to approximately 10^6 cells/ml.

Antibodies. Monoclonal anti-BrdUrd antibody identifies BrdUrd but not thymidine in ssDNA, free BrdUrd, or BrdUrd coupled to a protein carrier (Becton Dickinson, Product Information). HsRad51 protein, expressed in *E. coli*, was isolated and used for preparation of rabbit polyclonal antibodies (19). Western blotting experiments revealed that rabbit antiserum does not react significantly with any other proteins in mammalian cells except for Rad51 and its meiotic homolog DMC1. Because DMC1 is not detectable in fibroblasts using DMC1-specific antibodies (unpublished results), rabbit antiserum can be used as an immunofluorescent probe for Rad51 protein in somatic cells. Rabbit antiserum specifically directed against RPA was provided by James Ingles (University of Toronto). CREST autoimmune serum against centromeric proteins was used to label centromere dots during interphase (27).

Immunofluorescent Staining. Aliquots of 10^5 to 10^6 BrdUrd-substituted cells in suspension were centrifuged onto clean glass slides at $80 \times g$ for 4 min by using a Shandon Cytospin. Immediately after cytocentrifugation, the preparations were fixed in absolute methanol for 30 min at $-20°C$ and then rinsed in ice-cold acetone for a few seconds. To demonstrate BrdUrd incorporation into nuclear DNA, the slides were denatured in 70% formamide/2× SSC for 1 min at 80°C and then dehydrated in an alcohol series. BrdUrd was visualized by indirect immunofluorescence staining. First, the preparations were incubated with mouse monoclonal anti-BrdUrd antibody, diluted 1:50 with PBS, for 30 min. After three washes with PBS, they were incubated with Cy3-conjugated anti-mouse IgG (Dianova, Hamburg, Germany). For detecting ssDNA inside the nucleus, cytospin preparations of BrdUrd-substituted cells were processed for anti-BrdUrd immunofluorescence without a prior denaturation step. In some experiments, rabbit anti-Rad51, rabbit anti-RPA antiserum, or human CREST autoimmune serum was combined with anti-BrdUrd antibody. The slides were then incubated with fluorescein isothiocyanate-conjugated anti-rabbit IgG or anti-human IgG (Dianova) and Cy3-conjugated anti-mouse IgG, appropriately diluted with PBS. After three further washes with PBS, the preparations were counterstained with 1 μg/ml 4′,6-diamidino-2-phenylindole in 2× SSC for 5 min. The slides were mounted in 90% glycerol, 0.1 M Tris·HCl (pH 8.0), and 2.3% 1,4-diazobicyclo-2,2,2-octane.

Preparation of Chromatin Fibers. Aliquots of 10^6 cells were centrifuged onto glass slides and covered with 50 μl of 50 mM Tris·HCl (pH 8.0), 1 mM EDTA, and 0.1% SDS. After 0.5–1 min incubation with this detergent solution, the protein-extracted chromatin was mechanically sheared on the slide with the aid of another slide and then fixed in methanol and acetone (28, 29).

Fluorescence *in Situ* End Labeling (FISEL). After anti-BrdUrd antibody staining of ssDNA, preparations were thoroughly washed with PBS and processed further for the end-labeling reaction (26). Apoptotic cell death is detected by fluorescent labeling of the 3′ ends in fragmented genomic DNA with terminal deoxynucleotidyl transferase. Reaction mix (100 μl) contained 1 μl (25 units) terminal transferase (Boehringer Mannheim), 20 μl 5× cacodylate buffer (supplied with the enzyme), 1 μl 0.5 mM biotin-16-dUTP, 3 μl 0.5 mM dTTP, and 75 μl ddH$_2$O. Preparations were incubated at 37°C for 1 hr with this reaction mix. Washing the slides three times for 5 min in PBS is sufficient to

terminate the reaction. The incorporated biotin–dUTP was detected with fluorescein isothiocyanate-conjugated avidin (Vector Laboratories).

Digital Imaging Microscopy. Images were taken with a Zeiss epifluorescence microscope equipped with a thermoelectronically cooled charge-coupled device camera (Photometrics CH250), which was controlled by an Apple Macintosh computer. Gray scale source images were captured separately with filter sets for fluorescein isothiocyanate, Cy3, and 4′,6-diamidino-2-phenylindole. Gray scale images were pseudocolored and merged by using ONCOR IMAGE and ADOBE PHOTOSHOP software. Only signals that were clearly visible by eye through the microscope were scored to eliminate the possibility of false colocalizations caused by emission filter bleed through.

RESULTS

To visualize ssDNA *in situ*, we took advantage of the property of the base analog BrdUrd, which, when incorporated into DNA, interacts with anti-BrdUrd antibody, but only if the DNA is in the single-stranded form (30). In dsDNA the bromine atom is hidden in the phosphodiester backbone of the double helix and, therefore, is not accessible to the antibody. To incorporate BrdUrd in the place of thymidine into the nuclear DNA, cells were grown for one or two population doublings in the presence of BrdUrd. BrdUrd incorporation was visualized by indirect immunofluorescence staining with anti-BrdUrd antibody. After denaturation of the cell preparations, the vast majority (>90%) of nuclei from an exponentially growing culture displayed nearly uniform BrdUrd staining throughout the nucleus (data not shown; Fig. 1*G*), demonstrating that the entire nuclear DNA is more or less evenly labeled with BrdUrd. Cell preparations from the same culture, analyzed under nondenaturing conditions, did not show significant BrdUrd staining: 1% or less cells had discrete BrdUrd foci (Table 1). This indicates that BrdUrd in dsDNA is not efficiently bound by anti-BrdUrd antibody. The few ssDNA foci in untreated cells may represent a baseline frequency of endogenous ssDNA or be because the incorporated BrdUrd itself can cause DNA damage in the presence of light.

ssDNA as a Sensitive Cytological Marker for DNA Damage. Exposure of cells to γ irradiation or DNA-strand breakers (i.e., MMC and etoposide) resulted in a very rapid and dramatic increase (up to >50%) in the percentage of cells with BrdUrd foci (Table 1; Fig. 1*A*). Ionizing radiation induces mostly single-strand breaks and oxidized apurinic/apyrimidinic sites. These abasic sites are hydrolyzed by cellular endonucleases, thereby producing DNA-strand breaks (31). MMC cross-links DNA at guanine and adenine residues and disrupts base pairing (32). Topoisomerase II binds covalently to dsDNA, cleaves both strands, and reseals the cleaved complex. Etoposide interferes with this breakage and reunion cycle, trapping the enzyme in the cleaved complex. This results in irreparable DSBs (33). In addition, etoposide is a free radical generator.

Because BrdUrd foci were observed after DNA damage in nondenatured preparations, they evidently marked sites of ssDNA. When cells were exposed to γ irradiation or etoposide and analyzed at 1 hr after DNA damage, the percentage of cells with ssDNA foci increased in a dose-dependent manner (Table 1). The highest number of ssDNA-foci-positive cells was observed 1 hr after ^{60}Co irradiation or MMC treatment, with subsequent decreases at 6 hr and 24 hr. Two days after DNA damage, 5–10% of cells showed extremely bright and uniform nuclear staining with the anti-BrdUrd antibody, similar to that of denatured preparations. The same cells also stained FISEL positively (data not shown). FISEL quantifies apoptotic DNA-strand breaks by enzymatic labeling of the free 3′-OH ends with exogenous nucleotides. Cells with discrete ssDNA foci at 1–24 hr did not fluoresce after FISEL and, therefore, were not apoptotic. The kinetics of ssDNA-foci formation are consistent with the view that DNA-strand breaks are processed immediately after DNA damage to expose regions of ssDNA to repair proteins. Cells with
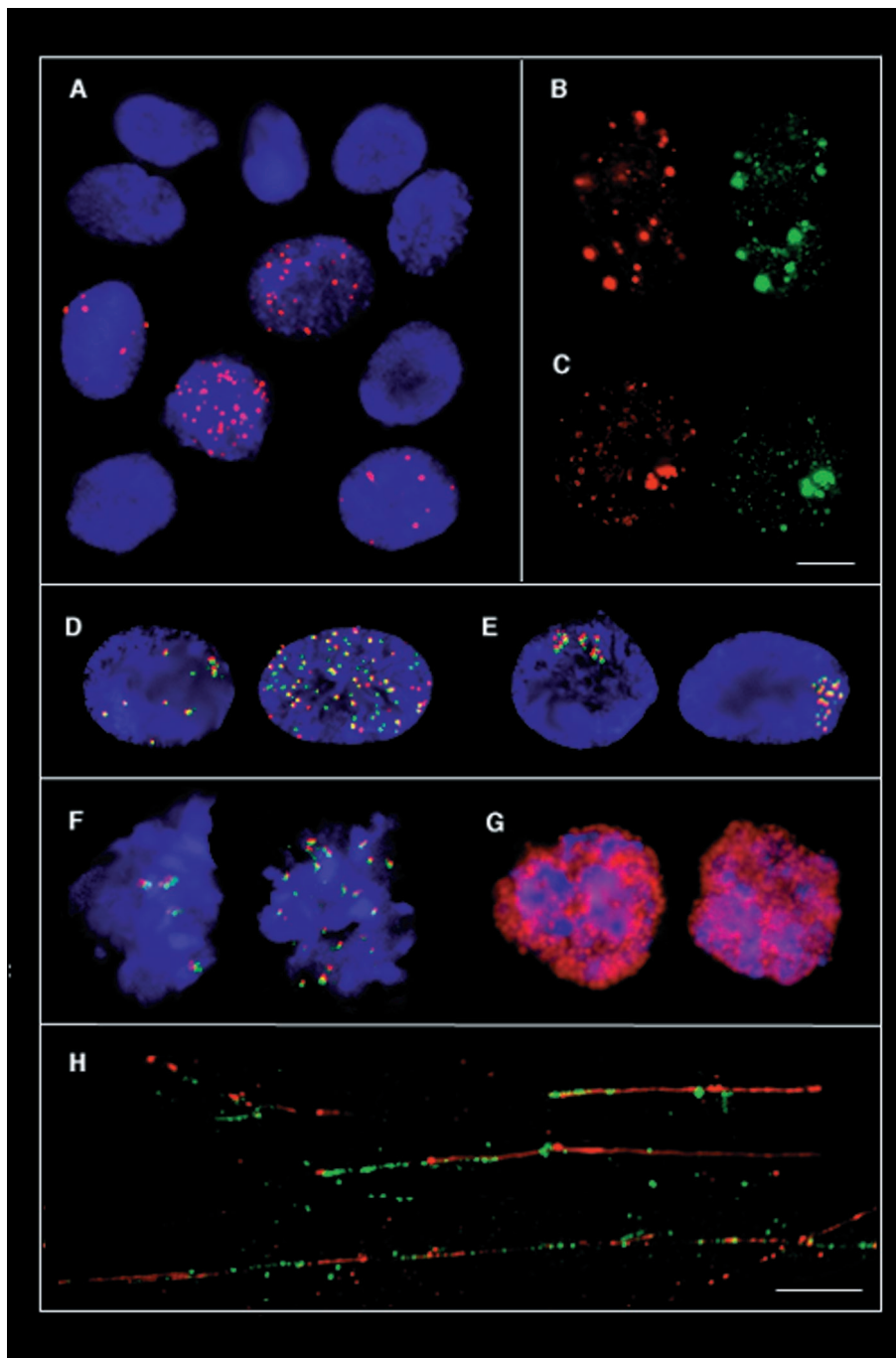
FIG. 1. Association of ssDNA foci with recombination proteins Rad51 and RPA. (*A*) Visualization of ssDNA foci in human PPL fibroblasts 1 hr after ^{60}Co irradiation with a dose of 10 Gy. Nuclear foci containing ssDNA are stained by red anti-BrdUrd antibody. Nuclei are counterstained with 4′,6-diamidino-2-phenylindole. At this time point, no Rad51 foci are seen. (*B* and *C*) Colocalization of Rad51 protein and ssDNA foci in PPL cells at 6 hr (*B*) and 24 hr (*C*) after irradiation. Nuclei on the left show ssDNA staining (red) and the nuclei at the right anti-Rad51 immunofluorescence (green) of the same cells. (*D* and *E*) Colocalization of replication protein A detected by anti-RPA antiserum (green) and ssDNA foci (red) at 6 hr (*D*) and 24 hr (*E*) after irradiation. To facilitate the demonstration of colocalizations, the green signals were shifted purposely by one pixel to the right and by one pixel to the bottom. (*F*) Colocalization of Rad51/DMC1 (green) and ssDNA (red) in mouse meiotic prophase cells. (*G*) As a control to demonstrate the uniform labeling of meiotic DNA with BrdUrd, anti-BrdUrd staining was performed on denatured spermatogenic cells. (*H*) Colocalization of Rad51 (green) and ssDNA (red) on experimentally stretched chromatin fibers from a γ-irradiated culture. Because individual cells are completely destroyed during preparation, the ssDNA fibers from the optical field shown do not necessarily represent the DNA from one cell. (Bars in *C* and *H* correspond to 10 μm.)

irreparable DNA damage accumulate large amounts of ssDNA during apoptotic genome fragmentation. Thus, similar to FISEL abundance of ssDNA inside the nucleus can be used as a death marker (34). To demonstrate the specificity of our assay, control cells were exposed to a lethal dose of the transcriptional inhibitor actinomycin D or the protein synthesis inhibitor cycloheximide. These two agents, which do not damage DNA directly, did not

cause a significant increase in the percentage of cells with ssDNA foci (Table 1).

Association of Rad51 and RPA with ssDNA Foci. Previously, we found that mammalian Rad51 changed its nuclear distribution after DNA damage and concentrated in discrete nuclear foci (19). Here we have used combined immunofluorescence staining of γ-irradiated cells with anti-Rad51 and anti-BrdUrd antibodies to

Table 1. Percentage of TGR-1 fibroblast nuclei containing ssDNA foci

Treatment	% Nuclei with ssDNA foci		
	Total	<10 Foci	>10 Foci
None	1	<1	<1
None	2	1	1
None	2	1	1
Denaturation	93	11	82
Cycloheximide (10 μg/ml) (for 1 hr)	2	1	1
Actinomycin D (100 ng/ml) (for 1 hr)	3	1	2
Etoposide (0.5 μg/ml) (for 1 hr)	32	23	9
Etoposide (2 μg/ml) (for 1 hr)	43	29	14
Etoposide (6 μg/ml) (for 1 hr)	57	33	24
Etoposide (20 μg/ml) (for 1 hr)	61	15	46
MMC (0.5 μg/ml) (for 1 hr)	36	12	24
3 hr after MMC	27	11	16
6 hr after MMC	33	14	19
15 hr after MMC	29	5	24
24 hr after MMC	32	11	21
48 hr after MMC	13	1	12
1 hr after 0.5 Gy	21	16	5
1 hr after 1 Gy	36	26	10
1 hr after 2 Gy	40	20	20
1 hr after 5 Gy	45	25	20
1 hr after 10 Gy	49	15	34
6 hr after 1 Gy	22	13	9
6 hr after 5 Gy	25	14	11
24 hr after 0.5 Gy	10	3	7
24 hr after 1 Gy	14	7	7
24 hr after 2 Gy	15	6	9
24 hr after 5 Gy	21	10	11
24 hr after 10 Gy	30	16	14

At least 300 nuclei were analyzed for each experiment.

demonstrate that Rad51 protein relocalizes to ssDNA foci in response to DNA damage (Fig. 1B). The percentage of cells with Rad51 foci increased after 3 hr, with a maximum at 24 hr. The majority of Rad51-foci-positive cells also displayed ssDNA foci (Table 2). Fifty to ninety percent of these cells with both ssDNA and Rad51 foci showed significant colocalizations, which means that more than 10% of the Rad51 foci in a given nucleus

overlapped with ssDNA foci. On average, more than 30% of foci in γ-irradiated fibroblasts were double-staining with anti-Rad51 and anti-BrdUrd antibodies (Table 3), whereas mock experiments using rabbit anti-Rad51 and human CREST antibodies yielded less than 5% double-staining foci, which are due to chance associations between Rad51 foci and centromeres. At 24 hr after irradiation, ssDNA–Rad51 foci were often clustered together in the periphery of the nucleus (Fig. 1C). This is consistent with the fact that the distribution of ssDNA–Rad51 foci is highly dynamic and dramatic nuclear reorganization occurs after DNA damage (20). Colocalizations of ssDNA and Rad51 foci with each other were also observed 24 hr after treatment with 10 μg/ml etoposide (Table 2).

Recently we found that Rad51 foci induced by DNA damage colocalized with RPA foci (35). Therefore, we performed combined immunofluorescent staining of RPA and ssDNA on γ-irradiated fibroblasts. In cells with both ssDNA and RPA foci, approximately 50% of the foci were double-staining (Table 3; Fig. 1 D and E). Thus, ssDNA foci not only contain Rad51 but also RPA that supports Rad51-mediated recombination (12, 16–18).

ssDNA–Rad51 Foci in Repair-Deficient Cells. XPA patients have defects in the enzyme that is responsible for lesion recognition by nucleotide excision repair and, therefore, accumulate DNA damage. The unexcised DNA lesions in XPA cells stimulate intrachromosomal homologous recombination (36, 37). Our assay indicated that these unexcised lesions lead to the formation of ssDNA and Rad51 foci, even without induction of DNA damage (Table 2). That a high percentage of ssDNA foci in XPA cells colocalized with Rad51 and RPA foci (Table 3), argues in favor of the notion that these are the nuclear sites where ssDNA–Rad51 filaments are formed.

ssDNA–Rad51 Foci in Meiotic Prophase Cells. To demonstrate that, in principle, the BrdUrd-labeling technique can also be carried out *in vivo*, we have visualized ssDNA during meiosis. Both the DSB and the ssDNA tail are obligatory intermediates in meiotic recombination (9, 38). The DNA of all spermatogenic cell types was substituted with BrdUrd by feeding male mice with BrdUrd containing water (25, 26). After denaturation of testicular cell preparations, the majority of premeiotic, meiotic, and postmeiotic cells showed strong overall BrdUrd labeling (Fig. 1G). When nondenatured preparations were stained with the anti-BrdUrd antibody, discrete foci containing ssDNA were visible in 5–10% of meiotic prophase cells (Fig. 1F). An average

Table 2. Induction of Rad51 and ssDNA foci by DNA damage

Cell line treatment	% Cells with				
	No foci	ssDNA foci (only)	Rad51 foci (only)	ssDNA and Rad51 foci*	
				Total	Co+
TGR-1					
24 hr after etoposide	15	42	5	38	19
PPL					
24 hr after etoposide	8	19	4	69	47
24 hr after 0.5 Gy	77	6	2	15	14
24 hr after 1 Gy	58	17	5	20	19
24 hr after 2 Gy	53	13	6	28	27
24 hr after 4 Gy	42	28	2	28	26
24 hr after 8 Gy	19	35	7	39	33
24 hr after 10 Gy	22	15	7	56	43
6 hr after 10 Gy	34	26	5	35	22
48 hr after 10 Gy	3	53	2	42	35
KRA					
24 hr after 10 Gy	28	18	9	45	30
XPA					
None	62	19	4	15	9

At least 300 cells were analyzed for each experiment.
*Co+ cells show >10% colocalization of Rad51 and ssDNA foci.

Table 3. Colocalization frequencies of ssDNA foci with Rad51 and RPA

Probe 1	Probe 2	PPL fibroblasts 24 hr after 10 Gy [No. (percent) of foci per nucleus stained with]			XPA fibroblasts without treatment [No. (percent) of foci per nucleus stained with]		
		1 and 2	1 only	2 only	1 and 2	1 only	2 only
Rad51	ssDNA	6.8 (35%)	5.4 (27%)	7.0 (38%)	10.7 (44%)	5.4 (22%)	8.2 (34%)
RPA	ssDNA	7.5 (50%)	3.7 (25%)	3.8 (25%)	9.5 (53%)	7.2 (41%)	1.1 (6%)
Rad51*	CREST*	0.7 (3%)	10.3 (52%)	8.7 (45%)	1.0 (4%)	10.4 (47%)	10.8 (49%)

50 cells with at least 5 foci of each type were analyzed for each double-staining (Rad51 and ssDNA, RPA and ssDNA, Rad51 and CREST) experiment.
*Because Rad51 foci and centromeres don't interact functionally, Rad51–CREST double-staining foci are caused by chance associations.

number of foci (17.2 ± 4.8) was counted in 50 ssDNA-positive cells. Simultaneous anti-Rad51 immunofluorescence demonstrated that meiotic ssDNA foci react with anti-Rad51 antibodies and, thus, are enriched with Rad51 and/or its meiotic homolog DMC1.

Association of Rad51 with Linear ssDNA Molecules. SDS lysis and mechanical stretching of nuclear chromatin across the surface of a glass slide can cause complete detachment of DNA loops from the nuclear matrix, producing highly elongated linear chromatin fibers (28, 29). Immunofluorescence staining of experimentally extended chromatin fibers from XPA and irradiated PPL fibroblasts revealed linear strings of ssDNA that were entirely or partially covered with Rad51 protein (Fig. 1*H*). PPL control cells exhibited a 5-fold lower number of ssDNA fibers per slide. In this context, it is important to note that SDS lysis, which is necessary to prepare chromatin fibers, may largely destroy protein epitopes and remove significant amounts of Rad51 protein from ssDNA. Therefore, it is not surprising that relatively few areas of a slide showed detectable Rad51 filaments. However, because the observed Rad51 filaments extensively overlapped with the linearized ssDNA, we conclude that these ssDNA–Rad51 fibers represent nucleoprotein filaments or stretched ssDNA–Rad51 foci.

Although the degree of chromatin stretching is not uniform along the length of a DNA fiber, DNA *in situ* hybridization experiments with clones of known size on similar preparations have revealed DNA extensions varying from 1 to 10 kb/μm (28, 29). Provided that ssDNA is not overstretched compared with dsDNA, the longest ssDNA filaments observed in both XPA and irradiated PPL cultures are estimated to be 50–100 kb. However, these extremely long ssDNA filaments may only represent a minor part of the DNA damage-induced ssDNA. Because a stretched ssDNA tail of 1 kb measures <1 μm, it would generate only a dot-like signal, which is almost indistinguishable from the relatively high background on fiber preparations.

DISCUSSION

Human Rad51 protein, a structural and functional homolog of *E. coli* RecA and *Saccharomyces cerevisiae* ScRad51, binds *in vitro* to ssDNA. The resulting nucleoprotein filament is considered to be the key element for promoting the pairing and strand exchange between ssDNA and homologous dsDNA (13–15). Our experiments demonstrate that a considerable percentage of nuclear Rad51 foci are formed at sites of DNA damage-induced ssDNA. Evidently, these Rad51 foci are the areas where Rad51 forms filaments on ssDNA inside the nucleus. Most models of recombination and repair involve a ssDNA intermediate. However, this is the first demonstration, *in situ*, of such an intermediate. Although significant colocalization is seen between Rad51 and ssDNA foci, the level of colocalization is always less than 100%. This is likely to reflect differences in the composition of recombination intermediates. Similar to meiotic recombination com-

plexes (39, 40), DNA damage-induced recombination intermediates may not have a set stoichiometry. In addition, single-staining foci may be due to technical problems, such as different epitope accessibility and limited sensitivity of the anti-Rad51 antiserum compared with anti-BrdUrd antibody.

Because generation of a dot-like fluorescence signal in the interphase nucleus requires the binding of at least 100 fluorescent antibody molecules (41), we estimate that the smallest detectable ssDNA foci must contain several kilobases of ssDNA, assuming that BrdUrd is randomly incorporated into DNA every 10th to 20th base pair. Obviously, such long stretches of ssDNA must be very rare in normally growing cell cultures. This explains why ssDNA (and Rad51) foci can be seen in only a small percentage of cells without DNA damage. The induction of ssDNA foci is a secondary event resulting from cellular responses to different types of clastogens. First, the initial DSB is processed by unidirectional 5′- to 3′-exonuclease digestion of one strand of each end to produce rather long 3′-overhanging ssDNA tails (38, 42, 43). These ssDNA tails may be used to search for homology and be involved in the invasion of homologous dsDNA. The ssDNA disappears as products are formed (9). Given that the estimated length of ssDNA tails associated with both meiotic and DNA damage-induced DSB repair is >1 kb, under optimal experimental conditions even a single DSB should be detectable by the anti-BrdUrd antibody technique. However, immunofluorescence assays are strongly biased toward detection of large accumulations of ssDNA and Rad51 protein. As a result, we may not be able to mark the majority of cells where DSBs are repaired by end-joining and homologous recombination. Most Rad51 filaments that are formed on ssDNA as intermediates of homologous recombination may be too short to be seen by immunofluorescence staining. Bright and easily detectable ssDNA–Rad51 foci may contain unusually large Rad51 filaments, which did not yet find a partner for homologous recombination and/or are irreparable.

The number (17.2 ± 4.8) of ssDNA foci in meiotic prophase cells was severalfold lower than the expected frequency of crossing-over events (44, 45). This discrepancy may be because of technical limitations, resulting in some underscoring of ssDNA–Rad51 foci. On the other hand, individual ssDNA foci may be short-lived and/or asynchrony in foci formation among different chromosomes may occur. In yeast meiosis, Rad51 (and DMC1) coincide with DSBs (46). Similar to our results, the maximum number of Rad51 foci in meiotic nuclei was 3- to 4-fold less than the number of recombination events. Recent observations on mouse meiocytes (21, 22, 47) suggest a much earlier, possibly premeiotic involvement of Rad51 in mammals. As meiotic prophase progresses, the Rad51 foci increase in size and decrease in number. This suggests that each ssDNA–Rad51 focus may contain several Rad51 filaments and, thus, mark sites of coalescing recombination intermediates during mammalian meiotic prophase.

Radiobiological data on DSB repair are consistent with a biphasic response of mammalian cells to DNA damage (48, 49). DSBs, which are repaired during the "fast" phase of DSB repair, most likely by nonhomologous end-joining, disappear within the first hour after irradiation. Cells responding with the "slow" system, which may involve homologous recombination, are repaired within 5 hr. The bulk ($\approx$80%) of DSB repair is completed at 1 hr after irradiation, when the maximum number of ssDNA foci is observed. At 3–24 hr after irradiation, when Rad51 protein accumulation is visible at ssDNA foci, relatively few (<5%) DSBs still persist. This strongly supports our conclusion that detectable ssDNA–Rad51 foci may contain unusually long Rad51–ssDNA-bound filaments. Indeed, measurements on extended chromatin fibers suggest that some filaments may contain up to 100 kb of ssDNA. Recently, we have shown that 1–2 days after γ irradiation the majority of these bright Rad51 foci coalesce and are removed into micronuclei, where the DNA is subject to apoptotic degradation (20). In addition, damage-sensitive regions are nonrandomly distributed in the highly substructured mammalian cell nucleus. For example, DNA lesions recognized by single-strand specific S1 nuclease are clustered in the genome (50). The extent and genomic distribution of DNA damage seems to depend on higher-order chromatin structure (51). Thus, clustering of multiple small Rad51–ssDNA-bound filaments may also account for the DNA damage-induced formation of foci with large amounts of ssDNA and Rad51 protein.

DSBs are repaired by two different recombination pathways, nonhomologous end-joining and homologous recombination. Yeast ScRad51, together with other members of the ScRad52 epistasis group, has been implicated in DSB repair (23, 24). Mammalian Rad51 protein, which closely resembles its yeast homolog in enzymatic activity (12–15), probably also contributes to DSB repair through homologous recombination. It was shown that the mammalian Mre11–Rad50 repair complex, which is likely to mediate nonhomologous end-joining (52, 53), migrates to the nuclear areas containing abundant DSBs, whereas Rad51 foci do not align with regions damaged by soft x-rays (54). However, it is entirely possible that soft x-ray treatment does not induce Rad51 foci at all. Our results clearly demonstrate that Rad51 foci assemble at sites of γ irradiation-induced DNA damage. In a conceptually related study (55), γ irradiation-induced Rad51 foci did not colocalize with Mre11–Rad50 foci. Indeed, Mre11–Rad50-positive cells never contained Rad51 foci (and *vice versa*), suggesting a cellular commitment to either nonhomologous end-joining or homologous recombination. One possible explanation for such a commitment may be the cell-cycle stage at which the cell experiences DNA damage. We conclude that Rad51 foci that are formed after DNA damage mark a subset of cells that have entered the homologous recombination pathway.

Homologous pairing and DNA-strand exchange, mediated by Rad51, is facilitated by human and yeast RPA (12, 16–18). Consistent with biochemical studies, we show DNA damage-induced association of RPA with ssDNA and Rad51 *in vivo*. Colocalization of Rad51 and RPA foci are also detected in yeast (39) and mammalian (40) meiotic cells at subnuclear structures that are thought to represent recombination nodules (21, 22). Taken together, we conclude that ssDNA–Rad51–RPA foci represent a repairosome-type assembly for recombinational DNA repair. Because ssDNA–Rad51–RPA foci are abundant after induction of DNA damage by various agents, homologous recombination seems to play an essential role in DSB repair in mammalian cells.

1. Wood, R. D. (1996) *Annu. Rev. Biochem.* **65,** 135–167.
2. Kuzminov, A. (1995) *Mol. Microbiol.* **16,** 373–384.
3. Jeggo, P. A. (1998) *Adv. Genet.* **38,** 185–218.
4. Bollag, R. J., Waldman, A. S. & Liskay, R. M. (1989) *Annu. Rev. Genet.* **23,** 199–225.
5. Lukacsovich, T., Yang, D. & Waldman, A. S. (1994) *Nucleic Acids Res.* **22,** 5649–5657.
6. Sargent, R. G., Brenneman, M. A. & Wilson, J. H. (1997) *Mol. Cell. Biol.* **17,** 267–277.
7. Taghian, D. G. & Nickoloff, J. A. (1997) *Mol. Cell. Biol.* **17,** 6386–6393.
8. Liang, F., Han, M., Romanienko, P. L. & Jasin, M. (1998) *Proc. Natl. Acad. Sci. USA* **95,** 5172–5177.
9. Osman, F. & Subramani, S. (1998) *Prog. Nucleic Acids Res. Mol. Biol.* **58,** 264–299.
10. Shinohara, A., Ogawa, H. & Ogawa, T. (1992) *Cell* **69,** 457–470.
11. Heyer, W. D. (1994) *Experientia* **50,** 223–233.
12. Sung, P. (1994) *Science* **265,** 1241–1243.
13. Benson, F. E., Stasiak, A. & West, S. C. (1994) *EMBO J.* **13,** 5764–5771.
14. Baumann, P., Benson, F. E. & West, S. C. (1996) *Cell* **87,** 757–766.
15. Gupta, R. C., Bazemore, L. R., Golub, E. I. & Radding, C. M. (1997) *Proc. Natl. Acad. Sci. USA* **94,** 463–468.
16. Benson, F. E. & West, S. C. (1997) *EMBO J.* **16,** 5198–5206.
17. Sugiyama, T., Zaitseva, E. M. & Kowalczykowski, S. C. (1997) *J. Biol. Chem.* **272,** 7940–7945.
18. Gupta, R. C., Golub, E. I., Wold, M. S. & Radding, C. M. (1998) *Proc. Natl. Acad. Sci. USA* **95,** 9843–9848.
19. Haaf, T., Golub, E. I., Reddy, G., Radding, C. M. & Ward, D. C. (1995) *Proc. Natl. Acad. Sci. USA* **92,** 2298–2302.
20. Haaf, T., Raderschall, E., Reddy, G., Ward, D. C., Radding, C. M. & Golub, E. I. (1999) *J. Cell Biol.* **144,** 11–20.
21. Ashley, T., Plug, A. W., Xu, J., Solari, A. J., Reddy, G., Golub, E. I. & Ward, D. C. (1995) *Chromosoma* **104,** 19–28.
22. Moens, P. B., Chen, D. J., Shen, Z., Kolas, N., Tarsounas, M., Heng, H. H. Q. & Spyropoulos, B. (1997) *Chromosoma* **106,** 207–215.
23. Shinohara, A. & Ogawa, T. (1995) *Trends Biochem. Sci.* **20,** 387–391.
24. Game, J. C. (1993) *Cancer Biol.* **4,** 73–83.
25. Ito, K., McGhee, J. D. & Schultz, G. A. (1988) *Genes Dev.* **2,** 929–936.
26. Smith, A. & Haaf, T. (1998) *BioTechniques* **25,** 496–502.
27. Haaf, T. & Schmid, M. (1989) *Hum. Genet.* **81,** 137–143.
28. Haaf, T. & Ward, D. C. (1994) *Hum. Mol. Genet.* **3,** 629–633.
29. Heiskanen, M., Karhu, R., Hellsten, E., Peltonen, L., Kallioniemi, O. P. & Palotie, A. (1994) *BioTechniques* **17,** 928–933.
30. Gray, J. W. (1985) *Cytometry* **6,** 501–673.
31. Demple, B. & Harrison, L. (1994) *Annu. Rev. Biochem.* **63,** 915–948.
32. Tomasz, M., Lipman, R., Chowdary, D., Pawlak, J., Verdine, G. L. & Nakanishi, K. (1987) *Science* **235,** 1204–1208.
33. Kaufmann, S. H. (1989) *Cancer Res.* **49,** 5870–5878.
34. Frankfurt, O. S., Robe, J. A., Sugarbaker, E. V. & Villa, L. (1996) *Exp. Cell Res.* **226,** 387–397.
35. Golub, E. I., Gupta, R. C., Haaf, T., Wold, M. S. & Radding, C. M. (1998) *Nucleic Acids Res.* **26,** 5388–5393.
36. Dasgupta, U. B. & Summers, W. C. (1980) *Mol. Gen. Genet.* **178,** 617–628.
37. Bhattacharyya, N. P., Maher, V. M. & McCormick, J. J. (1990) *Mol. Cell. Biol.* **10,** 3945–3951.
38. Sun, H., Treco, D. & Szostak, J. W. (1991) *Cell* **64,** 1155–1161.
39. Gasior, S. L., Wong, A. K., Kora, Y., Shinohara, A. & Bishop, D. K. (1998) *Genes Dev.* **12,** 2208–2221.
40. Plug, A. W., Peters, A. H. F. M., Keegan, K. S., Hoekstra, M. F., de Boer, P. & Ashley, T. (1998) *J. Cell Sci.* **111,** 413–423.
41. Haaf, T., Hayman, D. L. & Schmid, M. (1991) *Exp. Cell Res.* **193,** 78–86.
42. Sugawara, N. & Haber, J. E. (1992) *Mol. Cell. Biol.* **12,** 563–575.
43. Fishman-Lobell, J., Rudin, N. & Haber, J. E. (1992) *Mol. Cell. Biol.* **12,** 1292–1303.
44. Solari, A. J. (1980) *Chromosoma* **81,** 315–337.
45. Lawrie, M. N., Tease, C. & Hulten M. A. (1995) *Chromosoma* **104,** 308–314.
46. Bishop, D. K. (1994) *Cell* **79,** 1081–1092.
47. Plug, A. W., Xu, J., Reddy, G., Golub, E. I. & Ashley, T. (1996) *Proc. Natl. Acad. Sci. USA* **93,** 5920–5924.
48. Story, M. D., Mendoza, E. A., Meyn, R. E. & Tofilon, P. J. (1994) *Int. J. Radiat. Biol.* **65,** 523–528.
49. Lange, C. S., Mayer, P. J. & Reddy, N. M. S. (1997) *Radiat. Res.* **148,** 285–292.
50. Legault, J., Tremblay, A., Ramotar, D. & Mirault, M.-E. (1997) *Mol. Cell. Biol.* **17,** 5437–5452.
51. Roti Roti, J. L., Wright, W. D. & Taylor, Y. C. (1993) *Adv. Radiat. Biol.* **17,** 227–259.
52. Moore, J. K. & Haber, J. E. (1996) *Mol. Cell. Biol.* **16,** 2164–2173.
53. Schiestl, R. H., Zhu, J. & Petes, T. D. (1996) *Mol. Cell. Biol.* **14,** 4495–4500.
54. Nelms, B. E., Maser, R. S., MacKay, J. F., Lagally, M. G. & Petrini, J. H. J. (1998) *Science* **280,** 590–592.
55. Maser, R. S., Monsen, K. J., Nelms, B. E. & Petrini, J. H. J. (1997) *Mol. Cell. Biol.* **17,** 6087–6096.